Tetrahedron 64 (2008) 8394–8401

Contents lists available at ScienceDirect

Tetrahedron

journal homepage: www.elsevier.com/locate/tet

Investigations of rotamers in diaxial Sn(IV)porphyrin phenolates—towards a molecular timepiece

Sheshanath V. Bhosale, Connie Chong, Craig Forsyth, Steven J. Langford *, Clint P. Woodward

School of Chemistry, Monash University, Clayton Victoria 3800, Australia

ARTICLE INFO

Article history:
Received 10 March 2008
Received in revised form 21 May 2008
Accepted 30 May 2008
Available online 5 June 2008

Keywords:
Porphyrin
Coordination
Tin(IV)
Molecular dynamics
Rotamers
Supramolecular chemistry
Clock

ABSTRACT

An approach to the formation of molecular timepieces is outlined based on differentiating between rotamers in diaxial Sn(IV) porphyrin phenolates. Two models are explored in detail. The first explores how the rates of rotation of the diaxial ligands is discriminated based on steric hindrance of the two porphyrin macrocycle faces at low temperature. The second model explores a 'stopwatch' function based on the ligation of Ag(I) ions to a 5,15-dipyridylporphyrinato tin(IV) complex bearing 3-hydroxypyridine ligands. The complexation inhibits rotation of the axial ligand, a result, which can be reversed by precipitation of Ag(I) using tetraethylammonium bromide. X-ray crystallography has also been used to characterize two Ag(I) 5,15-dipyridylporphyrinato tin(IV)complexes. The two isoforms differ in their supramolecular organization. One structure is formed through a cofacial stack linking each porphyrin by Ag(I) coordination. The other displays a sheet-like coordination polymer structure.

1. Introduction

Mechanical devices that function as a result of the rotary motion of some component are common within our macroscopic world. Some familiar examples are helicopters, propellers, internal combustion engines, ATP synthase and flagellae to name but a few. In these cases, the rotation leads to mechanical work. However, rotational mechanical devices can also be used for measurement, typically as a result of (random) changes in rotary motion as derived from environmental stimuli including thermal energy. Examples here include gyroscopes, wind vanes and wind turbines, and indeed many macroscopic rotors have been demonstrated at a molecular level.[1,2]

One class of driven rotor is the analogue clock, stopwatch or timepiece—instruments that measure and record time with a dial.[3] In chemical terms, a timepiece is an entity that kinetically isomerizes through 86,400 dependent rotational isomers in a 24 h period. The dependency lies in the defined transition from one isomer to the next. Each of these rotational isomers, or rotamers, is measurable and hence instructive. Molecular rotamers, particularly displaying two states have been demonstrated elegantly in the fields of supramolecular chemistry.[4] Three example classes are the fluorescent molecular rotors,[5] the rotary motors of Feringa [6] and the catenanes of Sauvage[7] and Stoddart.[8] The latter system being used in a unique memory element for molecular based computing.[9] In each case, stimuli (e.g., electronic or photonic) produce a change in the system leading to the predominance of a new and different rotamer, which is addressable by spectroscopic means.

It occurred to us that the metalloporphyrin macrocycle, functionalized at all 12 outer peripheral positions could lead to a series of rotamers that mimic the basis of an analogue timepiece (Fig. 1). In this simple model, the four *meso* positions can be likened to the 3, 6, 9 and 12 positions of the timepiece. The eight remaining

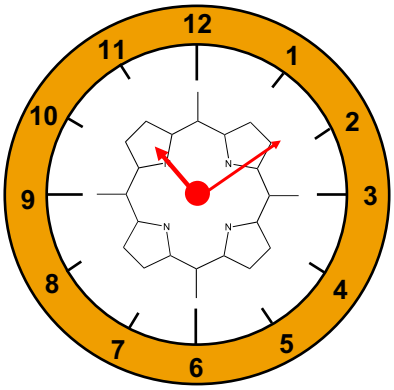

Figure 1. Metalloporphyrins bearing two axial ligands could conceivably act as a molecular timepiece in which the 12 positions around the porphyrin's outer periphery represent the 12 hourly positions on an analogue clock face.

* Corresponding author. Tel.: +61 3 9905 4569; fax: +61 3 9905 4597.
E-mail address: steven.langford@sci.monash.edu.au (S.J. Langford).

0040-4020/$ – see front matter © 2008 Elsevier Ltd. All rights reserved.
doi:10.1016/j.tet.2008.05.127

β-pyrrolic positions, which are evenly spaced between the *meso* positions, lead to the complete face numbering of the timepiece. The hands of the timepiece could be conceived from one or two axial ligands whose M–X–L bond angle (M=metalloporphyrin metal, X=heteroatom, L=ligand) is $90<^{\circ}<180$ to allow for circumnavigation of the porphyrin macrocycle and interaction with judicial functional groups around the outer periphery.

In terms of mobility, three aspects of the metalloporphyrin are important. The first is axial ligation, which leads to an axis upon which each ligand can rotate about the plane of the porphyrin. Secondly, the ability of *meso* groups, in particular, to rotate perpendicular to the porphyrin plane leading to atropisomerism. The third level of mobility is in the porphyrin plane itself in which ruffling or saddle formation is likely, leading to discrimination of regions around the macrocycle on geometric grounds. Of these, the former are more important from a design perspective.

2. The concept of a molecular timepiece

There are a number of design challenges to be addressed based on this concept:

(1) *The choice of metalloporphyrin*. In this case, diamagnetic metalloporphyrins that contain a metal ion centre with pseudo octahedral geometry would serve as the best candidates, though square pyramidal metal ions would also satisfy the definition of a clock. The strength of ligand binding should be such that ligand exchange is unlikely, especially under variable temperature conditions ($-60\ ^{\circ}C<T<60\ ^{\circ}C$) for pragmatic use. Hence association constants (K_a values) of $>10^5\ M^{-1}$ per ligand should be achieved.
(2) Controlling the motion of the axial ligands equates to the two arms of the timepiece. So discrimination of the dynamics of the two hands should be possible based on steric or electrostatic interactions.
(3) The ability to distinguish between the 12 positions of the face is required to allow for optimum addressability. In the easiest situation, distinguishing between the *meso* and β-pyrrolic positions represents the first challenge.
(4) Most analogue timepieces have the hands rotating in the same direction based on the internal mechanism. Similarly, for molecular motion to be useful it must be directional, leading from an initial state 'A' to a second state 'B', then a third 'C', etc. or at the very least, readable at each state.[4] Of greater challenge will be designing systems whereby the movement of one hand is dependent on the movement (and position) of the other.
(5) Finally, can stopwatch effects be employed, i.e., ways to control the STOP–START motion of the hands by restricting the rotation of one or both hands based on an external input?

In this paper, we describe two approaches that we hope advance the concept of a molecular timepiece. Our focus is on the use of Sn(IV) porphyrin phenolates to demonstrate this principle because of the inherent simplicity of this form of axial ligation and the flexibility in choice of phenolic ligand. More importantly, we know from previous work that both the fundamental requirements and that of concept (1) are satisfied in this class of metalloporphyrin.[10] Sn(IV) porphyrins are also advantageous in that their oxophilic character can be exploited as ways of imparting control over the dynamics of the ligands.[11]

3. An approach to control the dynamics of axial rotamers based on steric effects

In order to differentiate the two faces of a porphyrin by restricting rotation, an amount of steric bulk could be introduced to one face over the other as a thermodynamic barrier, but without totally impeding the desired rotational motion. One way of approaching this is to use monofunctional *meso* aryl groups (e.g., 2-methoxyphenyl units) antipodally displaced at any or all of the 5,10,15,20 positions of the porphyrin. Such functionalization, though, leads to a mixture of α and β atropisomers, which are either typically hard to separate or interconvert readily at ambient conditions. One way around this complication is to prepare porphyrins such as **1** bearing bulky methoxy groups at the 2,6-positions of one *meso* aryl group and a single and different substituents at the antipodal *meso* aryl group (Scheme 1). In this case, even if there is rotation about the *meso* aryl bond, the same structure is generated and atropisomerism is negated.

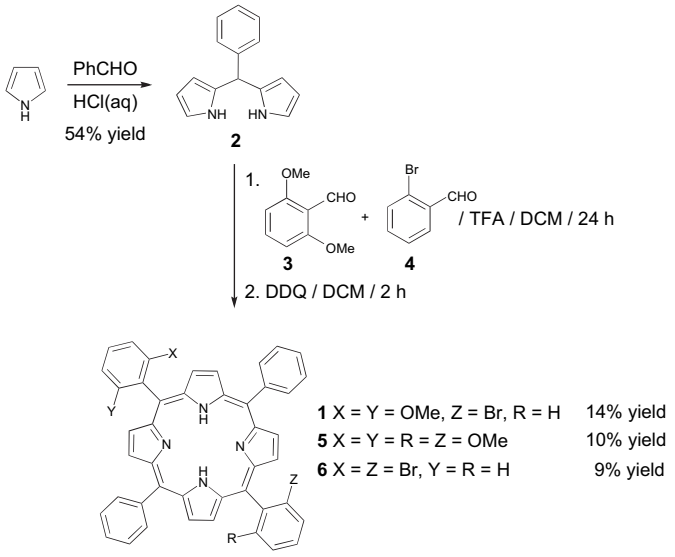

Scheme 1.

Porphyrin **1** was prepared as outlined in Scheme 1. Dipyrrylmethane **2** was prepared in 54% yield following modification of an existing method.[12] Dipyrrylmethane **2** was chosen because of its ease of synthesis, crystallinity and relative stability. Reaction of **2** with equimolar amounts of aldehydes **3** and **4** under acidic conditions leads to a mixture of porphyrinogens, which were not isolated but oxidized (DDQ) to a mixture of the corresponding porphyrins **1**, **5** and **6** in almost equivalent yields after chromatography. The fact that a statistical yield of porphyrins was not achieved indicates the interplay between the added reactivity of *ortho* electron donating aldehydes and the steric bulk of 2,6-disubstituted aldehydes in porphyrinogen formation. The judicial choice of methoxy substituents is also pragmatic, allowing easy separation of the complicated porphyrin mixture based by column chromatography and by giving a set of probe protons with which to monitor by NMR spectroscopy.

Oxidative insertion of the Sn(IV) metal centre in **1** (Scheme 2), **5** and **6** using stannous chloride in pyridine yields the dihydroxy Sn(IV) porphyrins **7**–**9**, respectively, in 88–93% yield.[14] Tin(IV)porphyrin phenolates[13] are the stable products of the equilibrium-based condensation reaction of substituted phenols with tin(IV)porphyrin dihydroxide in an organic medium. Condensation of **7** with **10** (2 equiv) in chloroform solution at reflux for 1 h (Scheme 2) yields the porphyrin phenolate complex in quantitative yield.

^{1}H NMR spectra of **7** and **7**·$\mathbf{10_2}$ are shown for comparison in Figure 2. Integration readily confirms the stoichiometry to be 2:1, consistent with the formation of **7**·$\mathbf{10_2}$ (Scheme 1).

The very large chemical shift changes ($\Delta\delta$) observed for the aromatic signals associated with the axial ligands in the complex **7**·$\mathbf{10_2}$ (>4 ppm in the case of *ortho* protons) are a result of the

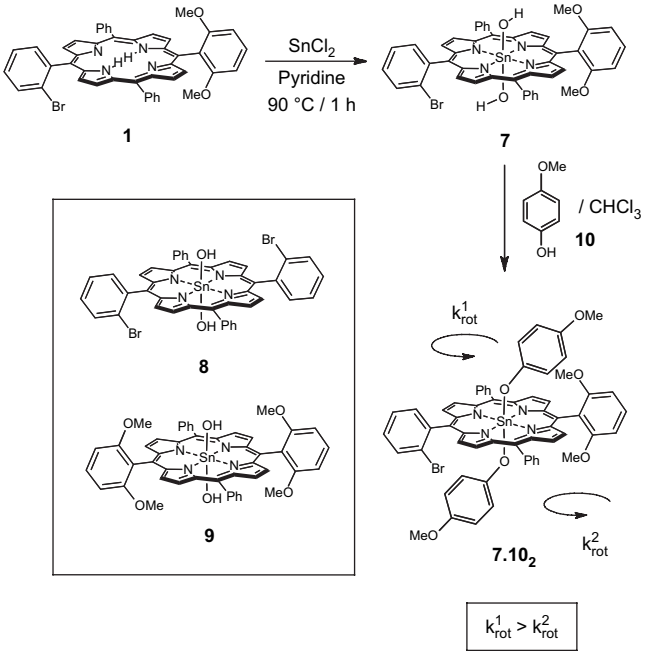

Scheme 2.

Table 1
Associated changes in chemical shift ($\Delta\delta$)[a] for selected probe protons for **7**·**10**$_2$, **11**·**12**$_2$ and [**11**·**12**$_2$·Ag_2]·2OTf in $CDCl_3$ solution at 300 K

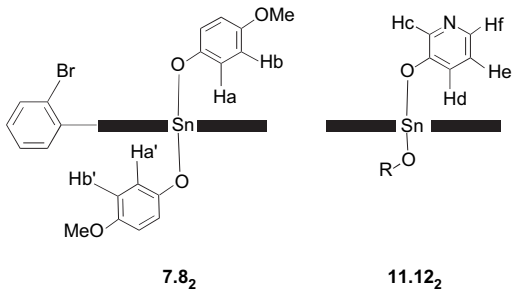

7.8$_2$ **11.12**$_2$

Attributed resonance	$\Delta\delta$ **7**·**10**$_2$	$\Delta\delta$ **14**·**12**$_2$	$\Delta\delta$ [**14**·**12**$_2$·Ag_2]·2OTf
H_a	−4.46	—	—
H_b	−1.51	—	—
$H_{a'}$	−4.64	—	—
$H_{b'}$	−1.54	—	—
H_c	—	−6.25	−0.27
H_d	—	−5.95	−0.48
H_e	—	−2.14	0.45
H_f	—	−0.61	0.21

[a] $\Delta\delta$=δ(complex)−δ(free phenol).

time-averaged orientation and proximity of these nuclei to the porphyrin ring current (Table 1). The changes are similar to that experienced for Sn(IV)TPP·**10**$_2$ in $CDCl_3$.[13] The aromatic region is also complicated, resolving each AA′ system of the β-pyrrolic protons due to the symmetry invoked by the antipodal *meso* substitution patterns. Evident are the two groups of signals at δ 1.9–2.2 and δ 5.2–5.4 attributable to the two different axial ligands as a result of their different environments based on 5,15-substitution patterns. The sharpness of each ^{1}H NMR signal at 400 MHz and 300 K indicates free rotation of the *p*-methoxybenzene ligands around the outer periphery. Warming the sample to 333 K (not shown) leads to identical spectra. Interestingly, cooling down incrementally to 240 K did not result in the expected broadening of ligand aromatic proton signals associated with the more hindered set (Fig. 2c). What is seen is the separation of OMe resonances of the ligand upon cooling, suggesting that at lower temperature, differentiation between these signals is achieved. The difference in broadness and height between the two signals may be indicative of the processes envisaged, though this is speculative. These changes are also accompanied by complication in the *meso* aryl proton resonances. Further cooling leads to significant broadening of the whole spectrum as a result of sample crystallization.

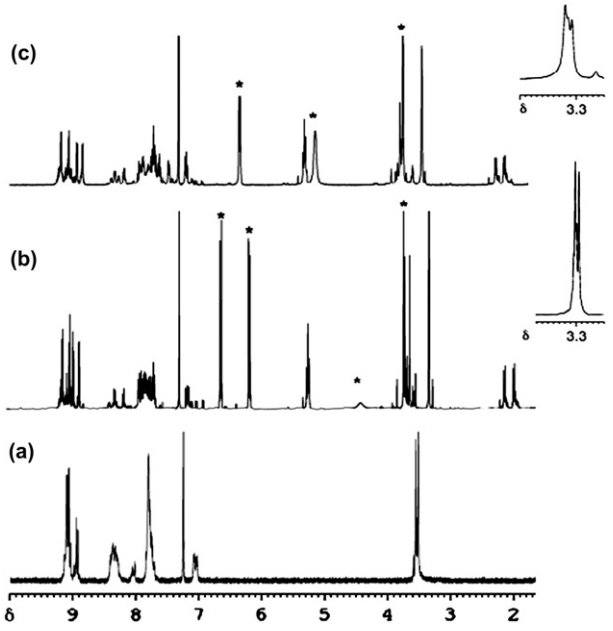

Figure 2. The 400 MHz ^{1}H NMR spectra of (a) **7** at 300 K and **7**·**10**$_2$ in $CDCl_3$ at (b) 300 K and (c) 240 K; * represents the *p*-methoxyphenol internal standard.

4. Controlling the dynamics of rotamers by metal ion coordination

The inconclusive nature of the results obtained using a steric approach and a means of better addressability for the different isomers formed prompted a change in design direction. Metal ion coordination can be used to dictate both the geometry of a ligand complex and also as a point of dynamic control.[11,15] Hence it seemed plausible to us that the rotation of axial ligands could be controlled in this manner to give a primitive stopwatch function or a means of controlling the rates of rotation. This second approach was based on the coordination of Ag(I) to a bipyridine ligand constituted from the 5,15-dipyridylporphyrin **11** and 3-hydroxypyridine **12** (Scheme 3). Porphyrin **13** was prepared from the dipyrrylmethane **2** and aldehyde **14** in 28% yield using the method already outlined in Scheme 1. Metallation of **13** ($SnCl_2$/Py/air) leads to the dihydroxy Sn(IV)porphyrin **11** in 91% yield. Condensation of **11** with **12** (2 equiv) in chloroform solution at reflux for 1 h yields the porphyrin phenolate complex **11**·**12**$_2$ in quantitative yield. Integration of the 300 MHz ^{1}H NMR spectrum readily confirms the stoichiometry of the complex formed between **11** and **12** to be 2:1. The sum of the porphyrin ring currents experienced by the protons on the pyridine linker again leads to large chemical shift changes in the ^{1}H NMR spectrum (Table 1). The changes are similar to that experienced for Sn(IV)TPP·**12**$_2$ in $CDCl_3$, therefore, we can conclude that no apparent interaction between the ligated and *meso* pyridines occurs.[13] Again, the sharpness of each ^{1}H NMR signal at 400 MHz and 300 K indicates free rotation of the axial pyridine ligands around the outer periphery (Fig. 3).

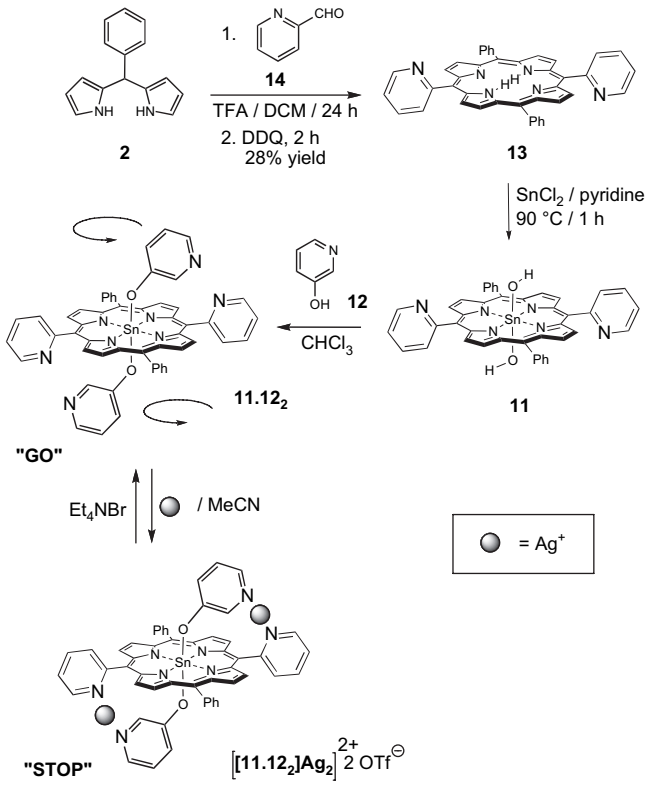

Scheme 3.

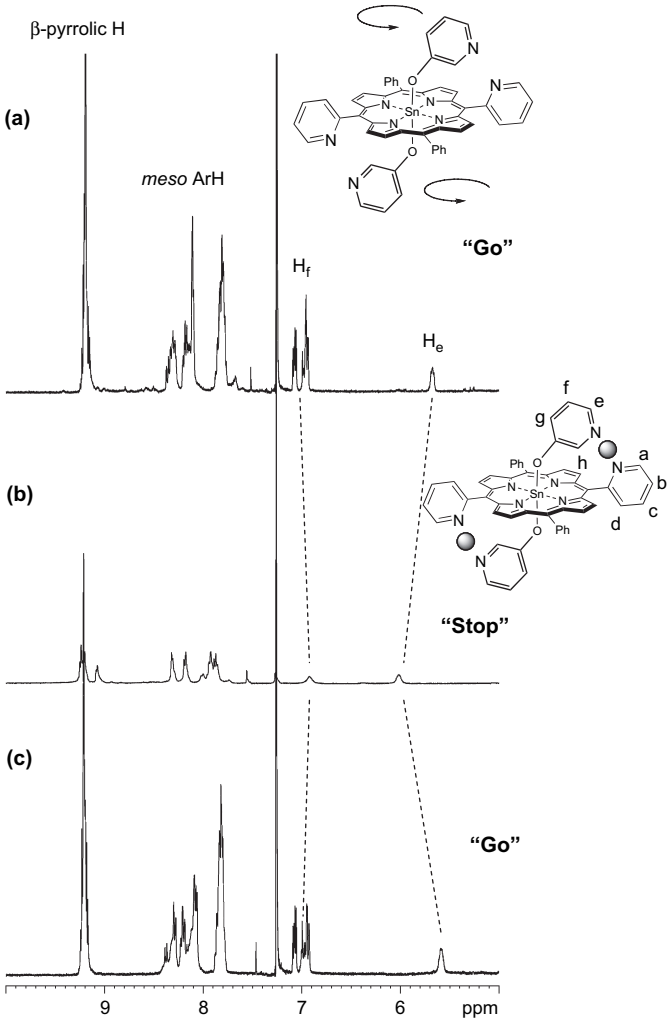

Figure 3. Partial 300 MHz ^{1}H NMR spectra of (a) **11**·**12**$_2$ at 300 K in $CDCl_3$, (b) after the addition of 2.2 equiv of AgOTf in MeCN and (c) after the addition of 2.2 equiv of Et_4NBr. The mode of binding shown in (b) is tentatively assigned based on NMR effects.

4.1. NMR studies on metal binding

Addition of 2.2 equiv of AgOTf to a solution of **11**·**12**$_2$ in MeCN-d_3 leads to a broadening of all signals and a concomitant change in chemical shifts for probe protons (Table 1) consistent with a change in the normal dynamics associated with **11**·**12**$_2$ at 300 K and 300 MHz (Fig. 3 a,b). The nature of this dynamics can be investigated further by variable temperature NMR studies at 400 MHz (Fig. 4). Cooling the solution from 300 to 293 K (Fig. 4f) leads to a sharpening of signals H_e and H_f, and further resolution into three unique forms in the ratio 1:2:1,[16] which persist to 243 K. Warming the solution to 323 K leads to a broadening of these probe protons and partial coalescence inferring restricted rotation on the NMR timescale being relaxed as a result of the elevation in temperature. Addition of 2.2 equiv of Et_4NBr to a solution of [**11**·**12**$_2$·Ag_2]·2OTf leads to decomplexation by the precipitation of AgBr and generation of the original spectrum of **11**·**12**$_2$ (Fig. 3c). Similar addition of AgOTf to a MeCN-d_3 solution of **7**·**10**$_2$, which is not capable of formal coordination, leads to no appreciable effect. In primitive terms, then, the results obtained for the addition of Ag^+ to **11**·**12**$_2$ lead to a situation of 'STOP–GO' control.

4.2. X-ray crystallographic studies on Ag(I) complexes

Dark red single crystals of **11**·**12**$_2$ suitable for X-ray crystallography were grown by treatment of **11**·**12**$_2$ with silver(I) trifluoroacetic acid in a 5:1 mixture of toluene and acetonitrile. Two crystal forms were isolated and subjected to X-ray crystallographic analysis. The two molecular structural isoforms of [**11**·**12**$_2$·Ag_2]·2OTf and the different macromolecular structures of the arrays formed are shown in Figures 5 and 6. In both cases, the metal centres of **11** are coordinated octahedrally via the four inner peripheral nitrogens of the porphyrin ligand and axially via the two phenolic oxygens (av. bond lengths: Sn–N=2.09±0.2 Å and Sn–O=2.05 Å). In each case, the phenolate groups lie in an *anti* orientation with respect to each other with an Sn–O–C angle of 122.2°.

In the case of Figure 5, a pseudo one-dimensional array is formed along the crystallographic *a*-axis in which the Ag(I) ion adopts a distorted tetrahedral geometry (N–Ag–N angles= 113.1<°<120.6) linking porphyrin units in a cofacial manner through a bipyridine arrangement defined as N_{meso}–Ag(I)–$N_{ligand'}$ (Fig. 5b). The tetrahedral geometry is further defined by a MeCN solvent molecule (Ag(1)–N(6) distance=2.515(10) Å) and a liberated 3-hydroxypyridine ligand (Ag(1)–N(5) distance=2.290(8) Å). The Ag–N_{ligand} (2.266(8) Å) and Ag–N_{meso} bonding distances (2.313(8) Å) are indifferent, which is surprising based on what one would reasonable assume is a negative inductive effect of the Sn(IV) centre, weakening the Ag–N_{ligand} bond. Solvent molecules (PhMe) sit within the voids between stacks in a unidirectional manner along the *b*-axis direction while the TfO^- counterions lie in a corrugated fashion in the direction of the *c*-axis.

Figure 6 shows the different isoforms, whose structure is dominated by a two-dimensional sheet array in which a zig-zag arrangement of porphyrin units is seen. The connectivity between porphyrins lies in two directions and is linked by Ag(I) ions in a distorted tetrahedral geometry (N–Ag–N angles=99.6<°<122.6) bearing three pyridine ligands (1×*meso* and 2×ligand) and a MeCN solvent molecule. The Ag–N bond distances are commensurate with the first structure. Disordered solvent (PhMe) and counterions

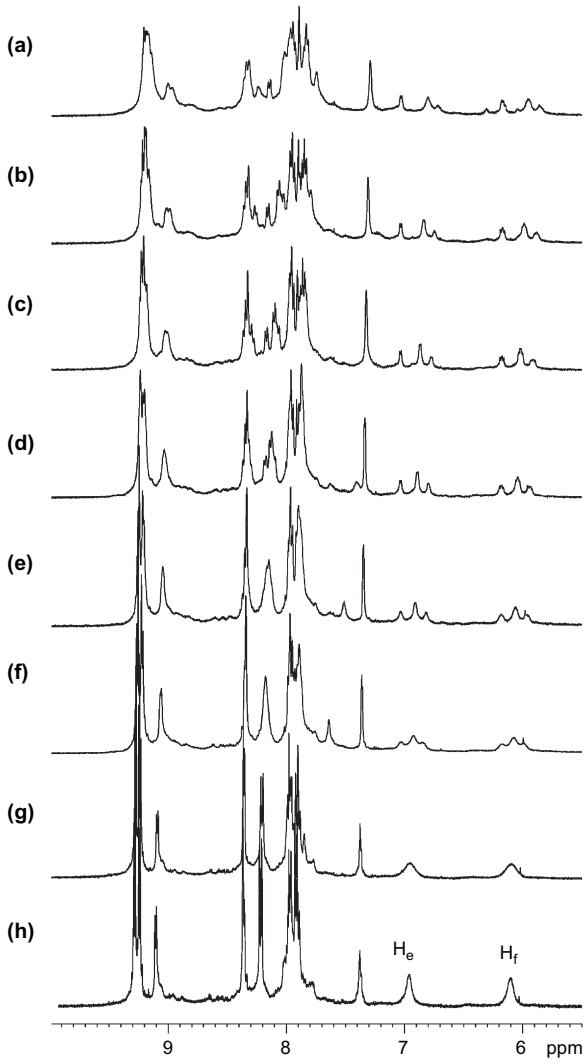

Figure 4. Variable temperature 400 MHz ^{1}H NMR spectra of [**11**·**12**$_2$·Ag_2]·2OTf in $CDCl_3$ (a) 243, (b) 253, (c) 263, (d) 273, (e) 283, (f) 293, (g) 313 and (f) 323 K.

sit in free spaces between the sheets with some measure of distortion.

The fact that in both cases an intermolecular interaction is observed over an intramolecular Ag(I) complex may be the result of both crystal packing forces and the method of preparation. As such, we do not believe that the coordination behaviour in the solid state is an accurate reflection of the Ag(I) binding mode in the NMR experiments conducted.

5. Outlook

An approach that mimics some aspects of the motion and control of a clock is outlined based on differentiating between rotamers in diaxial Sn(IV) porphyrin phenolates. Of the two models explored, exploitation of coordination or electrostatic interactions between the axial ligands and the *meso* positions of the porphyrin macrocycle (in the first instance) seems like a more plausible approach. This effect can be exploited in both a primitive stopwatch and to differentiate rotation of the axial ligands. Diffusion control is a complication for a pragmatic system though it has been used to demonstrate the principle in this case. The concern underlying a steric approach is the balance between restriction and impedance of motion. X-ray crystallography has also been used to characterize two Ag(I) 5,15-dipyridylporphyrinato tin(IV)complexes, though the

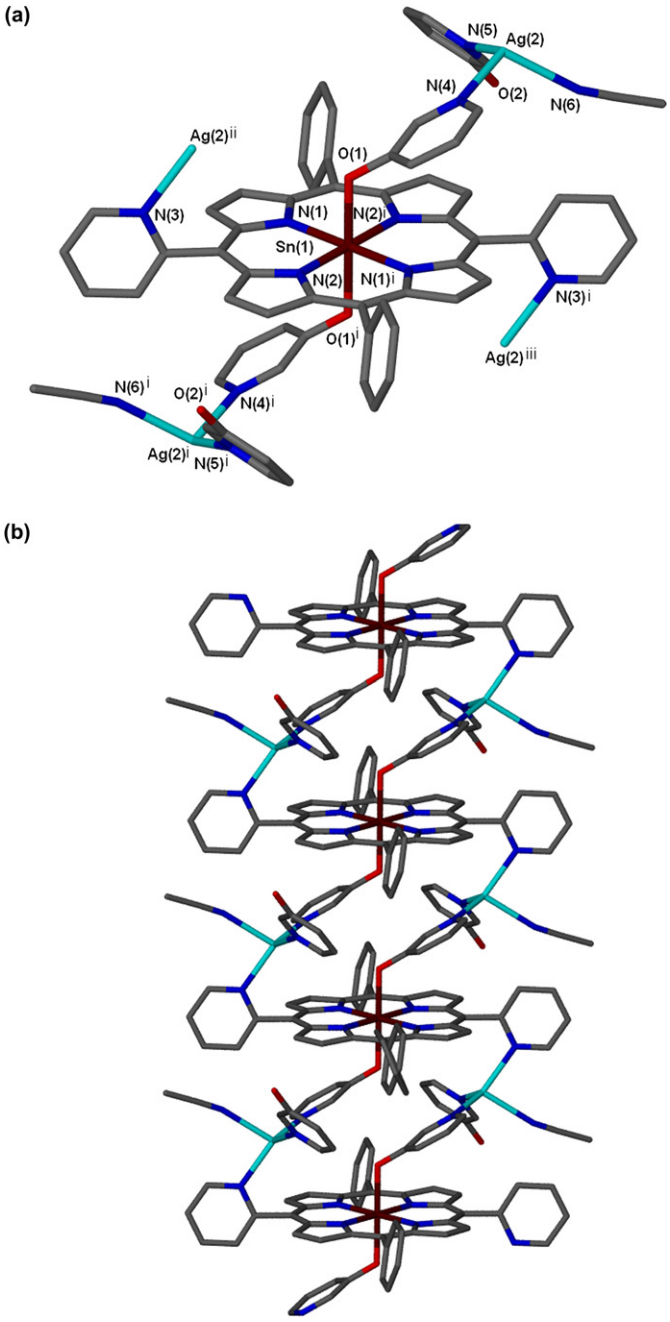

Figure 5. (a) Stick representation of part of the linear chain showing the Sn(IV) environment in [**11**·**12$_2$**·Ag_2]. Only one disordered component of the phenyl ring is shown. (b) View of an extended portion of the chain showing the Ag(I) coordination environment. Hydrogen atoms, lattice $CF_3SO_3^-$ anions and PhMe have been omitted for clarity.

coordination polymer topology obtained does not support the premise of the solution based results ideally. We are now in the process of developing new systems based on these results to advance this challenging area further.

6. Experimental section

6.1. General methods

All starting materials were purchased from Aldrich and used as-received. ^{1}H NMR spectra were recorded using the Bruker DPX 300 spectrometer operating at 300 and 75 MHz, and reference against

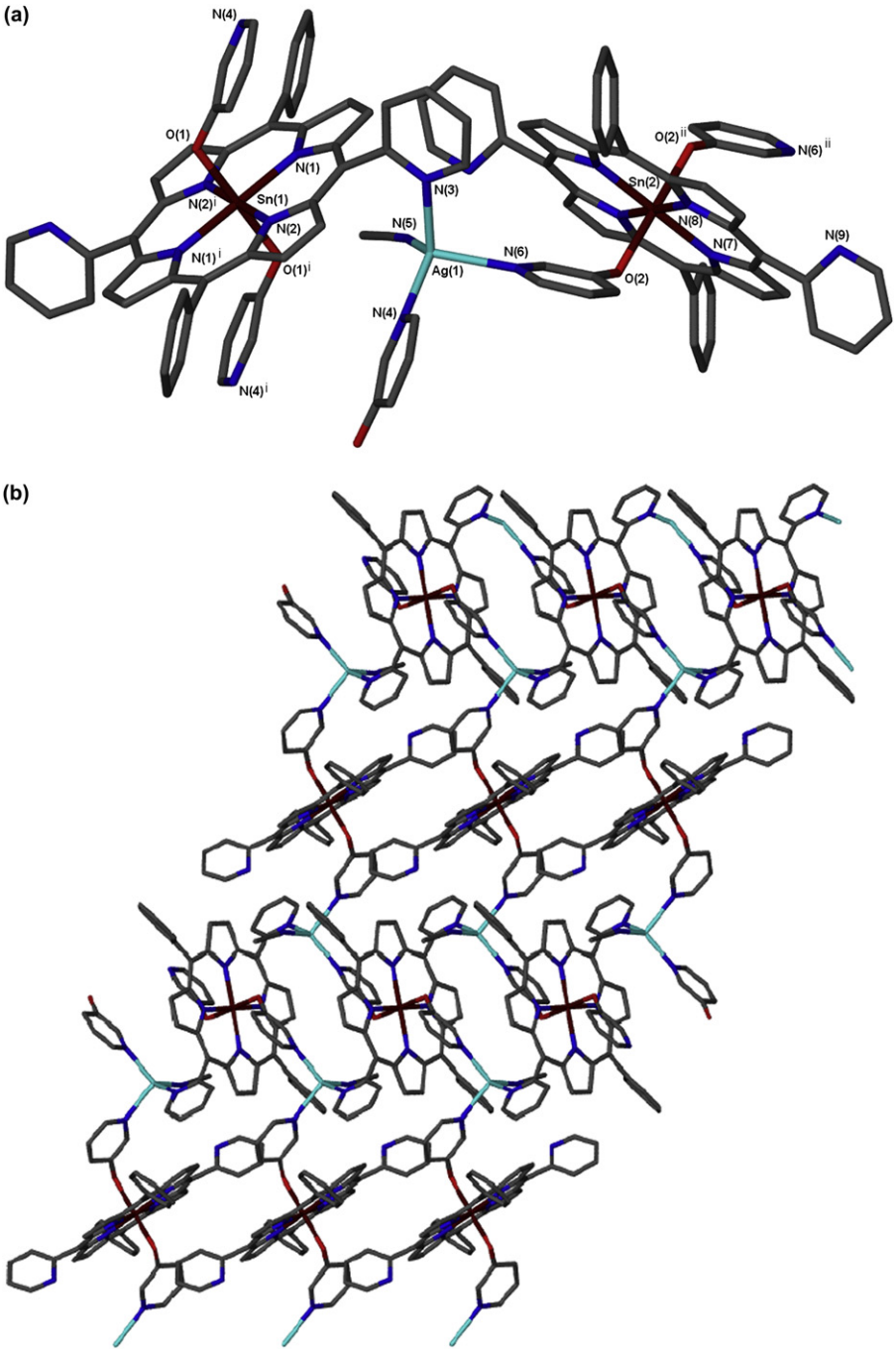

Figure 6. (a) Stick representation of part of the two-dimensional sheet of [**11**·**12**$_2$·Ag_2] showing the two unique Sn environments. Hydrogen atoms and the lattice CF_3SO_3 anion and PhMe have been omitted for clarity. (b) View of an extended portion of the two-dimensional sheet.

residual solvent ($CDCl_3$). Variable temperature studies were carried out on a Bruker DRX 400 spectrometer. High resolution mass spectra (HRMS) were recorded on an Agilent 6220 Accurate-Mass TOF LC/MS in positive-ion mode. X-ray crystallographic measurements were carried out using a Bruker Nonius X8 Apex II CCD diffractometer using graphite monochromatized Mo Kα radiation [λ(Mo Kα)=0.71069 Å] at 123.0±1 K. The cell constants and the orientation matrices for data collection were obtained from a least squares refinements. Structural solutions were obtained by direct methods (SHELXS-97)[17a] followed by successive Fourier-difference methods, and refined by full matrix least squares on F^2_{obsd} (SHELXL-97).[17b] The data were corrected for Lorentz and polarization effects and processed using Nonius software. Crystallographic data for the structural analyses have been deposited with the Cambridge Crystallographic Data Centre, CCDC 680785 and 680786 for structures of [**11**·**12**$_2$·Ag_2]·2OTf. Copies of this information may be obtained free of charge from The Director, CCDC, 12 Union Road, Cambridge, CB2 1EZ, UK (fax: +44 1223 336033; e-mail: deposit@ccdc.cam.ac.uk or http://www.ccdc.cam.ac.uk).

6.2. Synthetic procedures

6.2.1. 5-Phenyl-2,2′-dipyrrylmethane **2**[12]

A solution of benzaldehyde (2.0 mL, 20 mmol) and 20-fold excess pyrrole (28 mL, 400 mmol) were combined in a three neck round-bottom flask. The mixture was stirred in the dark at room

temperature under argon for 10 min followed by dropwise addition of trifluoroacetic acid (TFA, 0.5 mL). Completion of reaction was monitored by TLC; after 30 min stirring at room temperature the excess pyrrole was distilled and recovered. The crude product was purified by column chromatography on flash silica (40–60 mesh) eluting with CH_2Cl_2/hexane/Et_3N in the ratio of 100:50:1. Presence of dipyrrole was checked by TLC, under UV light, with dipyrrylmethane spots dark brown in appearance. The crude product was recrystallized from ethanol, giving **2** (54%, 2.78 g) as cream coloured crystals. Mp 101–102 °C (lit.:[12] 100–101 °C); ^{1}H NMR ($CDCl_3$, 300 MHz): δ 7.92 (br s, 2H), 7.22–7.32 (m, 5H), 6.71 (m, 2H), 6.14–6.18 (m, 2H), 5.92 (s, 2H), 5.48 (s, 1H); ^{13}C NMR (75 MHz, $CDCl_3$): δ 142.6, 133.2, 129.3, 128.9, 127.5, 117.7, 109.3, 107.8, 44.6. ESI-MS *m*/*z* 222 $(M+H)^+$.

*6.2.2. Synthesis of porphyrins **1**, **5** and **6***

5-Phenyl-2,2′-dipyrrylmethane **2** (0.70 g, 3.2 mmol), 2-bromobenzaldehyde (0.299 g, 1.6 mmol) and 2,6-dimethoxybenzaldehyde (0.265 g, 1.6 mmol) were dissolved in dichloromethane (400 mL) in a 1 L two neck round-bottom flask. Reaction mixture was stirred in the dark, under a slow stream of nitrogen for 30 min, and then trifluoroacetic acid (150 μL) was added via syringe in one portion. The reaction mixture was stirred for 24 h at room temperature, resulting in a dark red solution. A solution of 2,3-dichloro-5,6-dicyanobenzoquinone (800 mg) in 50 mL of dichloromethane was then added in one portion and the mixture stirred for an additional 2 h. The solvent was evaporated to dryness and the crude mixture was purified by column chromatography (SiO_2, DCM/acetone (98:2)). The fast moving fraction was identified as porphyrin **6**, the second band was identified as the target porphyrin **1** and the final band was identified as porphyrin **5**.

*6.2.2.1. Porphyrin **6**.* Yield: 9%, purple solid, mp >300 °C; ^{1}H NMR ($CDCl_3$, 300 MHz): δ 8.89 (d, *J*=4.5 Hz, 4H), 8.74 (d, *J*=5.1 Hz, 4H), 8.31–8.12 (m, 6H), 8.01 (m, 4H), 7.65–7.79 (m, 8H), −2.93 (s, 2H); ^{13}C NMR (75 MHz, $CDCl_3$): δ 160.8, 160.3, 144.5, 142.9, 142.6, 134.8, 132.2, 130.5, 130.2, 128.0, 127.8, 126.9, 126.8, 126.0, 120.8, 119.4, 118.6; UV–vis ($CHCl_3$) λ_{max} (nm, log ε)=419 (5.43), 514 (4.15), 549 (3.85), 589 (3.85), 646 nm (3.76); IR (ν_{max}, $CHCl_3$): 3695, 3035, 1471, 1005 cm^{-1}; HRMS-ESI *m*/*z* obsd 771.0751, calcd 771.0759 ($C_{44}H_{29}Br_2N_4$ $(M+H)^+$).

*6.2.2.2. Porphyrin **1**.* Yield: 14%, purple solid, mp >300 °C; ^{1}H NMR ($CDCl_3$, 300 MHz): δ 8.47 (m, 6H), 8.29 (d, *J*=5.1 Hz, 2H), 7.90–7.81 (m, 6H), 7.64 (br s, 1H), 7.45–7.32 (m, 8H), 6.76 (m, 2H), 3.21 (s, 3H), 3.14 (s, 3H), −3.05 (br s, 2H); ^{13}C NMR (75 MHz, $CDCl_3$): δ 160.7, 160.6, 143.1, 142.3, 135.2, 134.6, 132.0, 130.3, 129.8, 127.7, 127.6, 127.5, 125.8, 120.0, 119.6, 117.9, 112.9, 104.4; UV–vis ($CHCl_3$) λ_{max} (nm, log ε)=419 (5.53), 515 (4.26), 550 (3.88), 588 (3.90), 642 nm (3.73); IR (ν_{max}, $CHCl_3$): 3694, 3024, 3009, 2838, 1471, 1432, 1349, 1251, 1009 cm^{-1}; HRMS-ESI *m*/*z* obsd 753.1856, calcd 753.1865 ($C_{46}H_{33}BrN_4O_2$ $(M+H)^+$).

*6.2.2.3. Porphyrin **5**.* Yield: 10%, purple solid, mp >300 °C; ^{1}H NMR ($CDCl_3$, 300 MHz): δ 8.75 (s, 8H), 8.18 (m, 4H), 7.71 (m, 8H), 6.98 (s, 4H), 3.5 (s, 12H), −3.13 (s, 2H); ^{13}C NMR (75 MHz, $CDCl_3$): δ 160.9, 142.8, 134.8, 139.4, 127.7, 126.8, 121.8, 104.7, 104.6, 56.4; UV–vis ($CHCl_3$) λ_{max} (nm, log ε)=419 (5.47), 515 (4.21), 548 (3.87), 589 (3.89), 643 nm (3.77); IR (ν_{max}, $CHCl_3$): 3695, 3053, 3018, 2986, 2838, 1472, 1422, 1349, 1252, 1224, 1005 cm^{-1}; HRMS-ESI *m*/*z* obsd 735.2965, calcd 735.2971 ($C_{48}H_{38}N_4O_4$ $(M+H)^+$).

6.2.3. Typical experimental procedure for the preparation of tin complexes

The porphyrin (50 mg) and powdered $SnCl_2\cdot 2H_2O$ (40 mg) were stirred and refluxed in pyridine (20 mL) for 1 h. The solution was cooled to 50 °C, then concentrated NH_3 (5 mL) was added, and the resulting solution was stirred for 1 h. Water (30 mL) was added, and the solid collected by vacuum filtration, washed with water, and dried by suction filtration. The filter cake was digested in situ with chloroform (3×20 mL), which dissolved the purple product, leaving a brown residue of tin salts. The filtrate was dried over anhydrous Na_2SO_4 and concentrated to ~5 mL on a rotary evaporator. A column of alumina (20 g, neutral, activity V) was prepared in $CHCl_3$ and the concentrate was applied to the column and washed onto the alumina with a further 20 mL of solvent. The product was eluted with $CHCl_3$ and the purple band was concentrated (~3–5 mL). Hexane (20 mL) was carefully layered on top of the $CHCl_3$ solution, the flask stoppered and the mixture left to crystallize. The crystals were filtered, washed with hexane and dried in vacuum desiccators to give purple crystalline solid.

*6.2.3.1. Preparation of porphyrin **7**.* Yield: 93%, purple crystals, mp >350 °C; ^{1}H NMR ($CDCl_3$, 300 MHz): δ 9.11 (m, 6H), 8.95 (m, 2H), 8.38–8.33 (m, 6H), 7.82 (br s, 1H), 7.81–7.76 (m, 8H), 7.08 (m, 2H), 3.58 (s, 3H), 3.54 (s, 3H); ^{13}C NMR (75 MHz, $CDCl_3$): δ 160.7, 160.5, 152.9, 149.8, 147.6, 146.0, 140.8, 134.8, 134.6, 128.0, 126.6, 126.5, 118.0, 115.4, 114.4, 111.6, 111.5, 104.3, 104.2, 55.9, 55.8, 55.7, 55.2; UV–vis ($CHCl_3$) λ_{max} (nm, log ε)=429 (5.54), 561 (4.26), 600 nm (3.98); IR (ν_{max}, $CHCl_3$): 3627, 3043, 2946, 2837, 1485, 1422, 1260, 1213 cm^{-1}; HRMS-ESI (MeOH) *m*/*z* obsd 901.0826, calcd 901.0831 ($C_{47}H_{34}BrN_4O_3Sn$ $(M-2OH+OMe)^+$).

*6.2.3.2. Preparation of porphyrin **8**.* Yield: 89%, purple crystals, mp >350 °C; ^{1}H NMR ($CDCl_3$, 300 MHz): δ 9.16–9.09 (m, 4H), 9.00–8.94 (m, 4H), 8.37 (m, 6H), 7.83 (m, 2H), 7.82–7.79 (m, 10H); ^{13}C NMR (75 MHz, $CDCl_3$): δ 155.9, 155.7, 154.6, 154.3, 141.8, 141.3, 135.5, 135.2, 133.4, 132.7, 132.0, 130.9, 128.8, 128.7, 127.3, 127.3, 126.4; UV–vis ($CHCl_3$) λ_{max} (nm, log ε)=429 (5.48), 561 (4.15), 600 nm (3.88); IR (ν_{max}, $CHCl_3$): 3631, 3053, 2986, 1422 cm^{-1}; HRMS-ESI *m*/*z* obsd 903.9424, calcd 903.9495 ($C_{44}H_{26}Br_2N_4OSn$ $(M-OH)^+$).

*6.2.3.3. Preparation of porphyrin **9**.* Yield: 88%, purple crystals, mp >350 °C. ^{1}H NMR ($CDCl_3$, 300 MHz): δ 8.75 (br s, 8H), 8.37–8.32 (m, 4H), 7.80–7.76 (m, 8H), 7.08 (s, 2H), 7.02 (s, 2H), 3.53 (s, 12H); ^{13}C NMR (75 MHz, $CDCl_3$): δ 161.3, 160.9, 153.2, 150.8, 150.1, 148.0, 147.5, 147.4, 141.4, 135.0, 132.4, 131.7, 128.0, 126.7, 119.3, 118.5, 115.7, 114.7, 111.7, 104.6, 56.3, 56.1; UV–vis ($CHCl_3$) λ_{max} (nm, log ε)=428 (5.46), 560 (4.16), 600 nm (3.94); IR (ν_{max}, $CHCl_3$): 3585, 3026, 2932, 2840, 1472, 1422, 1252, 1205 cm^{-1}; HRMS-ESI (MeOH) *m*/*z* obsd 883.1925, calcd 883.1942 ($C_{49}H_{39}N_4O_5Sn$ $(M-2OH+OMe)^+$).

*6.2.4. Preparation of Sn(IV)(bis-p-methoxyphenolate) **7**·**10**$_2$*

The Sn(IV)porphyrin$(OH)_2$ complex **7** was added to 2 equiv of *p*-methoxyphenol **10** in base washed $CDCl_3$ and the solution was left to stir at 60 °C overnight. Yield: quantitative; ^{1}H NMR ($CDCl_3$, 300 MHz): δ 9.13 (d, *J*=7.9 Hz, β-pyrrolic-H_{Sn}, 2H), 9.06 (d, *J*=8.2 Hz, β-pyrrolic-H_{Sn}, 2H), 8.91 (d, *J*=7.9 Hz, β-pyrrolic-H_{Sn}, 2H), 8.79 (d, *J*=8.2 Hz, β-pyrrolic-H_{Sn}, 2H), 8.64–8.60 (m, *meso*-ArH_{Sn}, 3H), 7.91–7.62 (m, *meso*-ArH_{Sn}, 10H), 7.37 (m, *meso*-ArH_{Sn}, 4H), 5.25 (d, *J*=8.8 Hz, ArH, 2H), 5.18 (d, *J*=8.3 Hz, ArH, 2H), 3.61 (s, 6H), 3.54 (s, 6H), 2.17 (d, *J*=8.8 Hz, 2H), 1.92 (d, *J*=8.9 Hz, ArH, 2H); ^{13}C NMR (75 MHz, $CDCl_3$): δ 160.1, 147.0, 146.4, 141.0, 135.5, 135.4, 135.3, 135.2, 127.4, 127.4, 127.3, 126.5, 121.7, 121.4, 120.8, 119.8, 118.2, 115.3, 114.3, 111.4, 111.1, 105.6, 104.7, 56.2, 55.9, 55.8, 55.8, 55.7, 55.2; UV–vis ($CHCl_3$) λ_{max} (nm, log ε)=429 (5.56), 561 (4.28), 600 nm (3.89); IR (ν_{max}, $CHCl_3$): 3024, 2931, 2856, 1472, 1422, 1344, 1260, 1219 cm^{-1}; HRMS-ESI (MeOH) *m*/*z* obsd 901.0830, calcd 901.0831 ($C_{47}H_{34}BrN_4O_3Sn$ $(M-\mathbf{10}_2+OMe)^+$).

*6.2.5. 5,15-Bisphenyl-10,20-bis(2-pyridyl)porphyrin **13***

A round-bottom flask fitted with a rubber septum was charged with freshly distilled dichloromethane (320 mL) and purged with

bubbling Ar for 20 min. 5-Phenyl-2,2′-dipyrrylmethane **2** (0.65 g, 2.93 mmol) was added along with pyridine-2-carbaldehyde **14** (278 μL, 2.93 mmol) and the resulting solution was stirred for 30 min under Ar. Trifluoroacetic acid (150 μL) was added via syringe in one portion. The reaction mixture was stirred for 24 h at room temperature, resulting in a dark red solution. A solution of 2,3-dichloro-5,6-dicyanobenzoquinone (800 mg) in 50 mL of dichloromethane was then added in one portion and the mixture stirred for an additional 2 h. The solvent was evaporated to dryness and the crude mixture was purified by flash chromatography (DCM/methanol, 98.5:1.5), with the desired porphyrin **13** obtained in 28% yield (249 mg) as a purple solid. Mp >350 °C. ^{1}H NMR ($CDCl_3$, 300 MHz): δ −2.80 (s, 2H), 7.74 (m, 8H), 8.10 (t, J=6.9 Hz, 2H), 8.23 (m, 6H), 8.88 (d, J=9.9 Hz, 8H), 9.14 (d, J=3.9 Hz, 2H); ^{13}C NMR (75 MHz, $CDCl_3$): δ 161.1, 148.9, 142.4, 135.1, 135.0, 130.6, 128.0, 127.0, 122.7, 120.7, 118.9; UV–vis ($CHCl_3$): λ_{max} (nm, log ε)=407 (5.28), 502 (4.01), 536 (3.70), 576 (3.63), 628 (3.35); IR (ν_{max}, $CHCl_3$): 3696, 3023, 1464, 1427, 1005 cm^{-1}; HRMS-ESI obsd 617.2454, calcd 617.2448 ($C_{42}H_{28}N_6$ $(M+H)^+$).

*6.2.6. Preparation of [5,15-bisphenyl-10,20-bis(2-pyridyl)-porphyrinato]tin(IV)dihydroxide (**11**)*

5,15-Bisphenyl-10,20-bis(2-pyridyl)porphyrin **11** (50 mg) and powdered $SnCl_2\cdot 2H_2O$ (40 mg) were stirred and refluxed in pyridine (5 mL) for 1 h. The solution was cooled to 50 °C, then concentrated NH_3 (2.5 mL) was added and heated with stirring for 1 h. Water (30 mL) was added, and the solid collected by vacuum filtration, washed with water and dried by suction filtration. The filter cake was digested in situ with chloroform (3×10 mL), which dissolved the purple product, leaving a brown residue of tin salts. The filtrate was dried over anhydrous Na_2SO_4 and concentrated to ~10 mL on a rotary evaporator. A column of alumina (100 g, neutral, activity V) was prepared in $CHCl_3$ and the concentrate was applied to the column and eluted with $CHCl_3$, with the purple band concentrated (~3–5 mL) by rotary evaporation. Hexane (20 mL) was carefully layered on top of the $CHCl_3$ solution, the flask stoppered and the mixture left to crystallize. The purple crystals of **14** were filtered, washed with hexane and dried in vacuum desiccator. Yield (57 mg, 91%); mp >350 °C. ^{1}H NMR (300 MHz, $CDCl_3$): δ 9.21 (s, 8H, β-pyrrolic-H_{Sn}), 7.75–7.86 (m, 8H), 8.14–8.63 (m, 8H); ^{13}C NMR (75 MHz, $CDCl_3$): δ 159.5, 159.2, 149.3, 149.1, 146.6, 140.7, 135.5, 135.4, 135.2, 133.4, 133.3, 132.4, 130.9, 128.6, 127.3, 121.7, 121.6, 119.8; UV–vis ($CHCl_3$) λ_{max} (nm, log ε)=426 (5.48), 560 (4.22), 600 nm (3.86); IR (ν_{max}, $CHCl_3$): 3631, 3052, 3023, 2986, 1461, 1422, 1226, 1213 cm^{-1}; HRMS-ESI (MeOH) m/z obsd 765.1419, calcd 765.1425 ($C_{43}H_{29}N_6OSn$ $(M-2OH+OMe)^+$).

*6.2.7. Preparation of Sn(IV)(bispyridinephenolate) **11**·**12$_2$***

Sn(IV) porphyrin **11** (28.4 mg, 3.45 μmol) was added to 2 equiv of 3-hydroxypyridine (6.5 mg, 6.83 μmol) in base washed $CDCl_3$ and the solution was left to stir at 60 °C overnight. Yield: quantitative, purple solid, mp >350 °C. ^{1}H NMR (300 MHz, $CDCl_3$): δ 9.16 (s, 8H, β-pyrrolic-H_{Sn}), 7.86 (m, *meso*-ArH_{Sn}, 8H), 8.13–8.48 (m, 8H), 7.00 (d, J=1.3 Hz, 2H, ArH), 5.57 (m, 2H, ArH), 3.25 (d, J=2.7 Hz, 2H, ArH), 2.17 (m, 2H, ArH); ^{13}C NMR (75 MHz, $CDCl_3$): δ 213.0, 159.8, 159.5, 150.3, 149.6, 147.4, 146.8, 140.9, 139.1, 138.7, 135.2, 133.4, 133.2, 131.4, 130.9, 128.6, 124.2, 122.4, 121.7, 119.8, 113.4; UV–vis ($CHCl_3$) λ_{max} (nm, log ε)=426 (5.43), 560 (4.16), 599 nm (3.91); IR (ν_{max}, $CHCl_3$): 3024, 3005, 1462, 1428, 1005 cm^{-1}; HRMS-ESI (MeOH) m/z obsd 765.1424, calcd 765.1425 ($C_{43}H_{29}N_6OSn$ $(M-\mathbf{12}_2+OMe)^+$).

*6.2.8. Ag(I) NMR experiments with **11**·**12$_2$***

To a solution of Sn(IV)(bispyridinephenolate) **11**·**12$_2$** in $CDCl_3$ was added 2.2 equiv of silver triflate (AgOTf) in CH_3CN and the mixture stirred at room temperature for 2 h. The solvent was evaporated, the residual purple solid dissolved in $CDCl_3$ and their ^{1}H NMR spectra recorded at various temperatures. The addition of 2 equiv of Et_4NBr resulting in precipitation of AgBr leads to the spectrum corresponding to that of the free ligand Sn(IV)(bispyridinephenolate) **11**·**12$_2$**.

Acknowledgements

This work was funded under the Australian Research Council's Discovery project (DP0878220). One of the authors (S.J.L.) wishes to acknowledge Professor J. Fraser Stoddart for providing inspiration over a decade ago to always think 'outside the square'.

References and notes

1. (a) Kottas, G. S.; Clarke, L. I.; Horinek, D.; Michl, J. *Chem. Rev.* **2005**, *105*, 1281; (b) Khuong, T.-A. V.; Nunez, J. E.; Godinez, C. E.; Garcia-Garibay, M. A. *Acc. Chem. Res.* **2006**, *39*, 413; (c) Wintjes, N.; Bonifazi, D.; Cheng, F.; Kiebele, A.; Stöhr, M.; Jung, T.; Spillmann, H.; Diederich, F. *Angew. Chem., Int. Ed.* **2007**, *46*, 4089.
2. *Molecular Devices and Machines*; Balzani, V., Venturi, M., Credi, A., Eds.; Wiley VCH: Weinheim, 2003.
3. The term *clock* is a more general one for the sake of discussion, however, a quick search of chemical literature confuses the term with kinetic events such as the iodine clock. Hence the term *timepiece* is employed. Definitions come from Encarta® World English Dictionary © 1999 Microsoft Corporation.
4. (a) Magnera, T. F.; Michl, J. *Top. Curr. Chem.* **2005**, *262*, 63; (b) Kelly, T. R.; De Silva, H.; Silva, R. A. *Nature* **1999**, *401*, 150; (c) Kelly, T. R. *Acc. Chem. Res.* **2001**, *34*, 514; (d) Kay, E. R.; Leigh, D. A.; Zerbetto, F. *Angew. Chem., Int. Ed.* **2007**, *46*, 72.
5. (a) Haidekker, M. A.; Akers, W. J.; Fischer, D.; Theodorakis, E. A. *Opt. Lett.* **2006**, *31*, 2529; (b) Ghiggino, K. P.; Hutchison, J. A.; Langford, S. J.; Latter, M. J.; Lee, M. A. P.; Lowenstern, P. R. *Adv. Funct. Mater.* **2007**, *17*, 805; (c) Haidekker, M. A.; Brady, T. P.; Lichlyter, D.; Theodorakis, E. A. *J. Am. Chem. Soc.* **2006**, *128*, 398.
6. Feringa, B. *Acc. Chem. Res.* **2001**, *34*, 504.
7. Collin, J.-P.; Dietrich-Buchecker, C.; Gaviña, P.; Jiminez-Molero, M. C.; Sauvage, J.-P. *Acc. Chem. Res.* **2001**, *34*, 477.
8. Saha, S.; Stoddart, J. F. *Chem. Soc. Rev.* **2007**, *36*, 77.
9. Flood, A. H.; Peters, A. J.; Vignon, S. A.; Steuerman, D. W.; Tseng, H.-R.; Kang, S.; Heath, J. R.; Stoddart, J. F. *Chem.—Eur. J.* **2004**, *10*, 6558.
10. (a) Hawley, J. C.; Bampos, N.; Sanders, J. K. M.; Abraham, R. J. *Chem. Commun.* **1998**, 661; (b) Langford, S. J.; Lau, V.-L.; Lee, M. A. P.; Lygris, E. *J. Porphyrins Phthalocyanines* **2002**, *6*, 748.
11. A molecular gate based on a silver lock was recently reported. This system has the potential to function as a clock using the definitions invoked in this paper, see: Guenet, A.; Graf, E.; Kyritsakas, N.; Allouche, L.; Hosseini, M. W. *Chem. Commun.* **2007**, 2935.
12. Littler, B. J.; Miller, M. A.; Hung, C.-H.; Wagner, R. W.; O'Shea, D. F.; Boyle, P. D.; Lindsey, J. S. *J. Org. Chem.* **1999**, *64*, 1391.
13. Langford, S. J.; Lee, M. A.-P.; Macfarlane, K. J.; Weigold, J. A. *J. Inclusion Phenom.* **2001**, *41*, 135.
14. Arnold, D. P. *J. Chem. Educ.* **1988**, *65*, 1111.
15. Sato, D.; Akutagawa, T.; Takeda, S.; Noro, S.-I.; Nakamura, T. *Inorg. Chem.* **2007**, *46*, 363.
16. We are assuming that intramolecular complexation is faster than intermolecular complexation. The nature of the different magnetic environments is not known at this point though it could be as a result of different stereoisomeric forms induced by complexation.
17. (a) Sheldrick, G. M. *SHELXS-97*; University of Göttingen: 1997; (b) Sheldrick, G. M. *SHELXL-97*; University of Göttingen: Göttingen, 1997.